π-Arene/Cation Structure and Bonding. Solvation versus Ligand Binding in Iron(III) Tetraphenylporphyrin Complexes of Benzene, Toluene, *p*-Xylene, and [60]Fullerene

Daniel R. Evans,[†,§] Nathanael L. P. Fackler,[†,⊥] Zuowei Xie,[†,||] Clifton E. F. Rickard,[‡] Peter D. W. Boyd,*[,‡] and Christopher A. Reed*[,†]

Contribution from the Departments of Chemistry, University of California, Riverside, California 92521-0403, and The University of Auckland, Private Bag, Auckland, New Zealand

Received April 5, 1999. Revised Manuscript Received June 11, 1999

Abstract: Benzene, toluene, *p*-xylene, and [60]fullerene are shown to be weak ligands to a hard metal such as iron(III) in $Fe(TPP)^+$ cation (TPP = tetraphenylporphyrinate). X-ray crystal structures of $[Fe(TPP)(C_6H_6)][CB_{11}H_6Br_6]\cdot 3.5C_6H_6$ (**1**), $[Fe(TPP)(C_7H_8)][CB_{11}H_6Cl_6]\cdot 2C_7H_8$ (**2**), $[Fe(TPP)(C_8H_{10})][Ag(CB_{11}H_6Br_6)_2]\cdot$arene (**3**), and $[Fe(TPP)(C_{60})][F_{20}\text{-}BPh_4]\cdot 2.5$dichlorobenzene (**4**) show distinctively short Fe···C contacts, in the range 2.65−2.95 Å, which distinguish ligation from $\pi-\pi$ cocrystallized solvation. Dihedral angles between the arene and metalloporphyrin planes are also diagnostic of ligand versus solvate roles. The essential features of the arene coordination can be faithfully reproduced using density functional theory. In contrast to alkali metal cation/π-arene interactions, a component of the covalent bonding can be recognized. In a broader context, this study suggests that solvents such as benzene should always be viewed as potential ligands in the presence of coordinatively unsaturated cations. The common use in supramolecular chemistry of the term "noncovalent" to describe entities with metal−ligand bonds is viewed as misleading.

Introduction

The combination of modern theory and experiment is beginning to illuminate which fundamental forces are involved in the various classes of weak interactions of arenes with molecules and ions. Supramolecular chemistry,[1] crystal engineering,[2,3] protein structure,[4] enzymatic catalysis,[5] and organometallic catalysis[6] are some of the fields that will profit from a better understanding of these interactions.

The electron-rich nature of an arene HOMO lends itself to van der Waals, electrostatic, and covalent (donor) interactions. In the weak π bonding of arenes with hard metal cations, electrostatic forces typically predominate.[5] For example, approximately 60% of the binding energy of benzene to Na^+ is estimated to be electrostatic.[7] Induced dipoles are believed to be next most important. In the most well known of all weak arene interactions, face-to-face $\pi-\pi$ stacking or solvation, it is becoming clear that van der Waals forces alone do not account for their wide existence. Attractive $\sigma-\pi$ electrostatic forces, not easily recognized in nonpolar arenes because they are disguised as quadrupoles,[8] are important in defining the structures of $\pi-\pi$ interactions. Particular success has been encountered with porphyrins.[9] In the π interactions of arenes with soft, main group metals such as Ag^+ and Tl^+, some degree of covalent bonding must be important,[10,11] although the interaction remains relatively weak. The π complexation of arenes to phosphoazonium cations raises questions of electrostatic versus covalent contributions.[12] In the π complexation of electrophiles such as NO^+ to arenes, a charge-transfer interaction (i.e., covalence) is clearly an important component of the bonding.[13] In transition metal chemistry, η^2 π complexes of arenes to metals with partially filled d orbitals, e.g., $Os(NH_3)_5(arene)^{2+}$, can have strong covalent bonding.[14] In organic chemistry, electrophiles can show strong covalent bonding to arenes in σ complexes (so-called Wheland intermediates),[15] although in the case of $R_3Si(toluene)^+$ and $(C_6F_5)_3Al(toluene)$, it has been suggested that these structure should be viewed as points on a continuum of hybrid structures between (strong) σ and (weaker) π ideals.[16−18] Weak carbocation−π interactions have very recently received theoretical attention.[19]

* To whom correspondence should be addressed. E-mail: chris.reed@ucr.edu and pdw.boyd@auckland.ac.nz.
† University of California, Riverside.
‡ The University of Auckland.
§ Present address: University of Maryland.
⊥ Present address: Nebraska Wesleyan University.
|| Present address: Chinese University of Hong Kong.

(1) *Chem. Eur. J.* **1998**, *4*, 1349−1383 (special issue on supramolecular chemistry).
(2) Desiraju, G. R. *Angew. Chem., Int. Ed. Engl.* **1995**, *34*, 2311.
(3) Scudder, M.; Dance, I. *J. Chem. Soc., Dalton Trans.* **1998**, 3155.
(4) Burley, S. K.; Petsko, G. A. *Adv. Protein Chem.* **1988**, *39*, 125.
(5) Ma, J. C.; Dougherty, D. A. *Chem. Rev.* **1997**, *97*, 1303.
(6) Eisch, J. J.; Pombrik, S. I.; Zheng, G.-X. *Organometallics* **1993**, *12*, 3856.
(7) Mecozzi, S.; West, A. P., Jr.; Dougherty, D. A. *J. Am. Chem. Soc.* **1996**, *118*, 2307.
(8) Williams, J. H. *Acc. Chem. Res.* **1993**, *26*, 593.
(9) Hunter, C. A.; Sanders, J. K. M. *J. Am. Chem. Soc.* **1990**, *112*, 5525.
(10) Schmidbauer, H. *Angew. Chem., Int. Ed. Engl.* **1985**, *24*, 893.
(11) Basch, H. *Inorg. Chim. Acta* **1996,** *242*, 191.
(12) Burford, N.; Clyburne, J. A. C.; Bakshi, P. K.; Cameron, T. S. *Organometallics* **1995**, *14*, 1578.
(13) Kim, E. K.; Kochi, J. K. *J. Am. Chem. Soc.* **1991**, *113*, 4962.
(14) Harmon, W. D.; Taube, H. *J. Am. Chem. Soc.* **1987**, *109*, 1883.
(15) (a) Reed, C. A.; Fackler, N. L. P.; Kim, K.-C.; Stasko, D.; Evans, D. R.; Boyd, P. D. W.; Rickard, C. E. F. *J. Am. Chem. Soc.* **1999**, *121*, 6314. (b) Rathore, R.; Hecht, J.; Kochi, J. K. *J. Am. Chem. Soc.* **1998**, *120*, 13278.
(16) Reed, C. A.; Xie, Z.; Bau, R.; Benesi, A. *Science* **1993**, *262*, 402.
(17) Reed, C. A. *Acc. Chem. Res.* **1998**, *31*, 325.

10.1021/ja9910816 CCC: $18.00
Published on Web 09/03/1999

In a recent X-ray crystal structure, the first to apparently contain the long sought "free" $Fe(TPP)^+$ ion (TPP = tetraphenylporphinate),[20] we observed a close interaction of an iron(III) porphyrin with a cocrystallized *p*-xylene molecule, derived from the solvent. Some features of the structure were typical of $\pi-\pi$ solvation, but the short $Fe\cdots C_{arene}$ distance (2.89 Å) and the canting of the arene plane relative to the porphyrin plane (dihedral angle 13°) suggested the beginnings of η^2 metal−ligand covalent bonding. The structure was significantly different from that of $[Mn(TPP)(H_2O)][SbF_6]\cdot$benzene, where the solvating arene was nearly coplanar with the porphyrin and the shortest Mn−C distance was 3.32 Å.[21] This raised the question of whether the arene in the iron complex was acting as a solvate or a ligand (or both). A few further questions arise: How well does molecular structure reflect the different bonding modes, and are they distinct? Although such bonding is obviously very weak, does it have a covalent component? If so, what are the relative contributions of van der Waals, electrostatic, and covalent bonding? In this paper, we explore these questions via systematic X-ray structural investigations on new weak complexes of $Fe(TPP)^+$ with arenes and with C_{60}, together with calculations using nonlocal density functional theory.

Results and Discussion

Synthesis and Structure. Hexahalocarborane anions, $CB_{11}H_6X_6^-$ (X = Cl, Br), or their silver complex ions, $[Ag(CB_{11}H_6X_6)_2]^-$, are very weakly coordinating anions with Lewis basicities similar to those of common arenes.[22] As a result, we can expect solvents such as benzene and toluene to compete with these anions for a vacant coordination site. In a labile system such as Fe(TPP)Y (Y = weakly coordinating anion), the solution equilibrium of eq 1 can be biased to either side by crystal forces during crystallization.

$$Fe(TPP)Y + \text{arene} \rightleftharpoons Fe(TPP)(\text{arene})^+ + Y^- \qquad (1)$$

By systematic variation of the anions, the nature of the arene solvent, and crystallization conditions, it is possible to isolate X-ray-quality single crystals of most of the possible combinations of neutral and ionic complexes. The neutral compounds $Fe(TPP)(CB_{11}H_6Br_6)$ and $Fe(TPP)(Ag(CB_{11}H_6X_6)_2)$ will be reported in a future publication,[23] in connection with their interesting magnetochemical properties.[24] Crystals of the ionic species with benzene in $[Fe(TPP)(C_6H_6)][CB_{11}H_6Br_6]\cdot 3.5C_6H_6$ (**1**) and with toluene in $[Fe(TPP)(C_7H_8)][CB_{11}H_6Cl_6]\cdot 2C_7H_8$ (**2**) have been isolated from benzene and toluene solutions, respectively. Their structures can be compared with those of the previously isolated *p*-xylene-containing species $[Fe(TPP)(C_8H_{10})][Ag(CB_{11}H_6Br_6)_2]\cdot$arene (**3**). In addition, we have crystallized a fullerene adduct, $[Fe(TPP)(C_{60})][F_{20}\text{-}BPh_4]\cdot$2.5dichlorobenzene (**4**), which shows a very short Fe···C contact.

Arene solvent interactions with $Fe(TPP)^+$ seem to be necessary for the crystallization of ionic rather than neutral complexes. They apparently displace the coordinated anion and fill lattice space to keep the anions and cations well separated. This dual role is illustrated for benzene in the structure around the $Fe(TPP)^+$ cation in **1** (see Figure 1). The relationship of the two close-approaching benzene molecules to the cation suggests that one is primarily a ligand, while the other is a solvate. For the ligated benzene (top in Figure 2), the closest Fe···C approach is short (2.82 Å), and the Fe atom is 0.16 Å out of the mean plane of the 24-atom porphyrin core toward it. The plane of the benzene ring is canted by 14.4° with respect to the mean porphyrin plane. The other benzene is farther away from the iron atom (shortest Fe···C = 3.18 Å) and is canted by 31.1° from the porphyrin plane. These features are similar to those of the corresponding *p*-xylene structure,[20] which also had one close-approaching and one more distant arene. The occurrence of guest molecules above and/or below the plane of four-coordinate TPP complexes (i.e., the formation of clathrates) is a highly conserved feature of tetraarylporphyrin lattices and is driven by the difficulty of packing symmetrical bulky objects efficiently.[25]

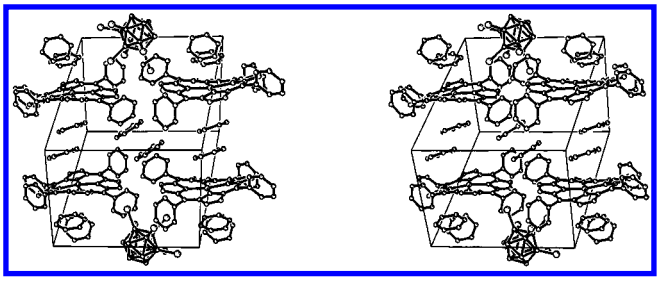

Figure 1. Stereoscopic packing diagram for $[Fe(TPP)(C_6H_6)][CB_{11}H_6Br_6]\cdot 3.5C_6H_6$ (**1**).

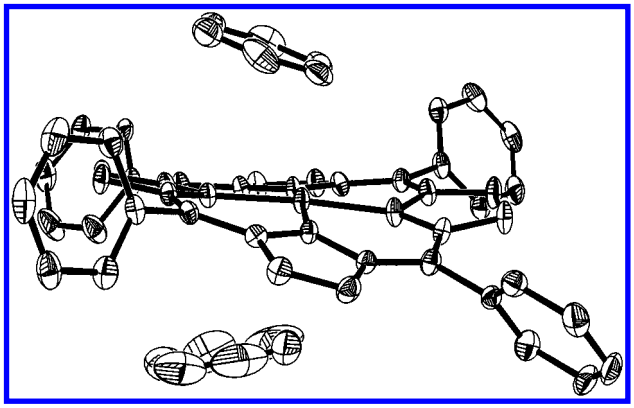

Figure 2. Relationship of the two benzene molecules to the $Fe(TPP)^+$ cation in **1**.

The corresponding structure with toluene is somewhat different. As shown in Figure 3, only one arene molecule is incorporated within close proximity to the ferric ion. It clearly takes a ligand role (shortest Fe···C = 2.71 Å), but instead of a second solvating arene in the vicinity of the sixth coordination site, the porphyrin adopts a slipped face-to-face relationship with itself. This is a common structural motif for four- and five-coordinate porphyrin complexes, and the mean interplanar separation of 3.53 Å is typical.[26]

Table 1 compares the metric parameters for close-approaching benzene, toluene, and *p*-xylene interactions with $Fe(TPP)^+$ in **1**, **2**, and **3**. In each case, the arene can be viewed as an η^2 ligand. The average Fe−C distance increases in the nonhomologous order toluene < benzene < *p*-xylene, suggesting that

(18) Hair, G. S.; Cowley, A. H.; Jones, R. A.; McBurnett, B. G.; Voigt, A. *J. Am. Chem. Soc*. **1999**, *121*, 4922.
(19) Miklis, P. C.; Ditchfield, R.; Spencer, T. A. *J. Am. Chem. Soc*. **1998**, *120*, 10482.
(20) Xie, Z.; Bau, R.; Reed, C. A. *Angew. Chem., Int. Ed. Engl.* **1994**, *33*, 2433.
(21) Williamson, M. M.; Hill, C. L. *Inorg. Chem.* **1987**, *26*, 4155.
(22) Reed, C. A. *Acc. Chem. Res.* **1998**, *31*, 133.
(23) Evans, D. E.; Reed, C. A. Submitted for publication.
(24) Reed, C. A.; Guiset, F. *J. Am. Chem. Soc.* **1996**, *118*, 3281.
(25) Byrn, M. P.; Curtis, C. J.; Hsiou, Y.; Khan, S. I.; Sawin, P. A.; Tendick, S. K.; Terzis, A.; Strouse, C. E. *J. Am. Chem. Soc.* **1993**, *115*, 9480.
(26) Scheidt, W. R.; Lee, Y. J. In *Structure and Bonding*; Springer-Verlag: Berlin, 1987; p 1.

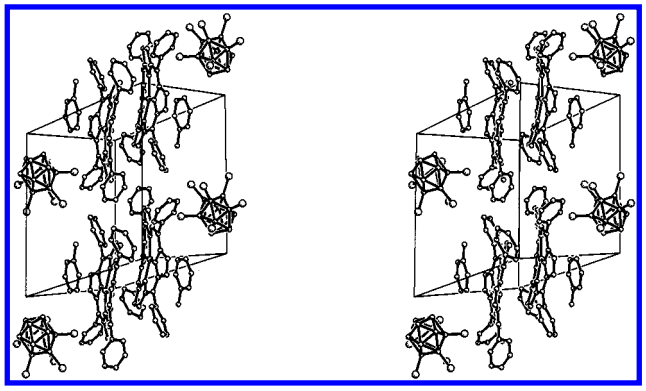

Figure 3. Stereoscopic packing diagram for $[Fe(TPP)(C_7H_8)][CB_{11}H_6Cl_6]\cdot 2C_7H_8$ (**2**).

Table 1. Summary of Structural Parameters for $[Fe(TPP)(Arene)]^+$ in Complexes **1**, **2**, and **3** and for $Fe(TPP)(C_{60})^+$ in **4**

	benzene	toluene	*p*-xylene	C_{60}
Fe−C (Å)	2.817, 2.878 (av 2.85)	2.710, 2.927 (av 2.82)	2.948, 2.948 (av 2.95)	2.570, 2.690, 3.082, 3.143
$Fe-N_{av}$ (Å)	1.959 (10)	1.974 (3)	1.975 (4)	1.974(4)
$Fe\cdots Ct_P$[a] (Å)	0.16	0.15	0.07	0.015
$\angle P_{24}\cdots Ar$[b]	14.4°	16.4°	12.6°	−

[a] Ct_P = Center of least-squares plane defined by the 24-atom porphyrin core (P_{24}). [b] Ar = Least-squares plane defined by the six carbon atoms of the ligated arene core.

the stronger electronic interactions expected for the more electron-rich arenes are outweighed by steric effects once two methyl groups are attached to the benzene. The average iron−nitrogen distance in these complexes is 1.97 (1) Å. This is comparable to the shortest reported value in an iron(III) tetraphenylporphyrin complex, that of 1.961 (5) Å in the carborane anion-coordinated species $Fe(TPP)(CB_{11}H_{12})$.[27] The shortness of the Fe−N distances reflects the weakness of the arene interactions and suggests a very close approach to a "pure" $S = {}^3/_2$ spin state expected for the bare $Fe(TPP)^+$ cation, i.e., where there is complete depopulation of the antibonding $d_{x^2-y^2}$ orbital, whose lobes are directed along the Fe−N bonds.[23] $Fe(TPP)(CB_{11}H_{12})$ has been analyzed in terms of an admixed $S = {}^3/_2$, ${}^5/_2$ spin state, with 92% $S = {}^3/_2$ contribution.[27]

The small size of the iron atom, compared to the relaxed porphyrin hole size, is responsible for the saddle-shaped ruffling of the porphyrin cores seen in all three structures.[26] As can be seen in the displacement diagrams shown in Figure 4, the particular pattern of ruffling appears to be influenced by steric effects from the arene methyl groups in the toluene and *p*-xylene structures. Because the ruffling leads to local variations in planarity of the porphyrin core, we do not attempt to put a fine interpretation on the trend in the dihedral angles (cant angles) between the ligand arene planes and the porphyrin mean planes. In fact, the canting is remarkably similar in all three structures ($15 \pm 3°$). Similarly, local effects make it difficult to place any interpretation on the cant angles of the lattice-filling solvate arenes. Small, local electrostatic influences are likely to control the particular orientation of weak $\pi-\pi$ interactions with some of these lattice solvates, and, because of packing inefficiencies, they can take unpredictable orientations.

Calculated Molecular Structures. The molecular and electronic structures of the cationic porphine complexes $[Fe(porphine)]^+$, $[Fe(porphine)(benzene)]^+$, $[Fe(porphine)(toluene)]^+$, and $[Fe(porphine)(p\text{-xylene})]^+$ have been investigated using density functional theory. It has recently been shown that this method gives the appropriate delocalized structures for the porphyrin moiety,[28−32] whereas Hartree−Fock theory leads to structures corresponding to frozen resonance forms.[33] The calculations include electron correlation, which is an important part of the description of the electronic structure of iron porphyrins.[34]

(i) $[Fe(porphine)]^+$. A full geometry optimization of the $[Fe(porphine)]^+$ cation using nonlocal density functional methods indicates that the lowest energy state for this system is the intermediate spin state, $S = {}^3/_2$. The energies of the $S = {}^1/_2$ and $S = {}^5/_2$ states lie 0.31 and 1.36 eV, respectively, above the ground state. The computed geometry of the $S = {}^3/_2$ complex has D_{4h} symmetry. The iron atom sits in the plane of the porphyrin ring. The Fe−N bond length of 1.96 Å is consistent with expectations for an intermediate spin planar iron(III) complex based on the spin state−structure correlations of Scheidt and Reed.[35] For the $S = {}^5/_2$ and $S = {}^1/_2$ structures, the Fe−N distances are calculated to be 2.03 and 1.97 Å, respectively. The other bond distances and angles agree well with reported data for iron metalloporphyrins.[28]

(ii) $[Fe(porphine)(benzene)]^+$. The molecular geometry of $[Fe(porphine)(benzene)]^+$ was optimized with the iron atom in the intermediate $S = {}^3/_2$ spin state. The benzene molecule binds to the iron atom in an η^2 fashion, and, with no symmetry restraints, the Fe−C distances are 2.81 and 2.76 Å. The overall point group symmetry of the complex is close to C_s. Optimization of the complex using a model with imposed C_s symmetry gives a structure of insignificantly different energy (0.23 kcal/mol). The iron atom lies 0.16 Å out of the mean plane of the porphine toward the benzene carbon atoms, with an Fe−C distance of 2.79 Å. The average Fe−N distance is 1.97 Å. The benzene molecule is canted with respect to the porphine plane by 14.8°. The benzene C−C bond η^2 with respect to the iron atom (1.392 Å) is lengthened relative to that calculated for isolated benzene (1.381 Å). The binding energy of the benzene molecule to the iron porphyrin cation was calculated to be −14.6 kcal/mol.

(iii) $[Fe(porphine)(toluene)]^+$ and $[Fe(porphine)(p\text{-xylene})]^+$. The molecular geometries of the toluene and *p*-xylene complexes of iron porphine were calculated as above. In the toluene complex, there are two possible η^2 bonding situations. One has the ortho and meta carbon atoms binding to the iron atom, while the other, as found experimentally, has the meta and para carbon atoms bound. Calculation shows that both modes are possible and that only a 0.2 kcal/mol difference exists between them, indicating the flatness of the arene−iron porphyrin potential surface. In the *p*-xylene complex, the C−C bonds to the methyl groups lie parallel to an N−Fe−N vector, and the ortho and meta carbon atoms are bound to the iron atom in an η^2 mode (Figure 5). This is the same as what is observed experimentally. In both the toluene and xylene cases, the dimensions of the iron porphyrin moiety and the orientation of the arene are similar to those calculated for the $[Fe(TPP)(benzene)]^+$ cation.

(27) Gupta, P. G.; Lang, G.; Lee, Y. J.; Scheidt, W. R.; Shelly, K.; Reed, C. A. *Inorg. Chem.* **1987**, *26*, 3022.
(28) Matsuzawa, N.; Ata, M.; Dixon, D. A. *J. Phys. Chem.* **1995**, *99*, 7698.
(29) Delley, B. *Physica B* **1991**, *172*, 185.
(30) Obara, S.; Kashiwagi, H. *J. Chem. Phys.* **1982**, *77*, 3155.
(31) Jones, D. H.; Hinman, A. S.; Ziegler, T. *Inorg. Chem.* **1993**, *32*, 2092.
(32) Ghosh, A.; Almlöf, J.; Que, L. *J. Phys. Chem.* **1994**, *98*, 5576.
(33) Almlöf, J.; Fischer, T. H.; Gassman, P. G.; Ghosh, A.; Häser, M. *J. Phys. Chem.* **1993**, *97*, 10964.
(34) Kuramochi, H.; Noodleman, L.; Case, D. A. *J. Am. Chem. Soc.* **1997**, *119*, 11442.
(35) Scheidt, W. R.; Reed, C. A. *Chem. Rev.* **1981**, *81*, 543.

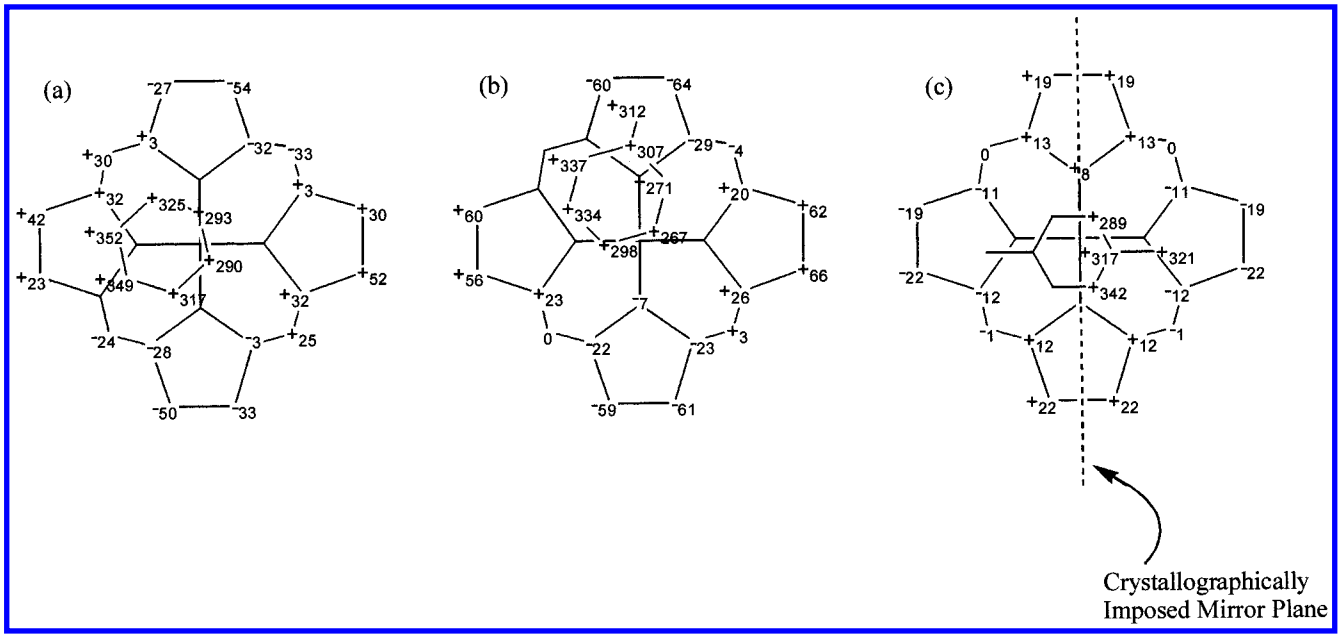

Figure 4. Displacements (in 10^{-3} Å) of atoms from the mean plane of the 24-atom porphyrin core for (a) benzene complex **1**, (b) toluene complex **2**, and (c) *p*-xylene complex **3**. Positive values are for atoms above the plane, negative values below.

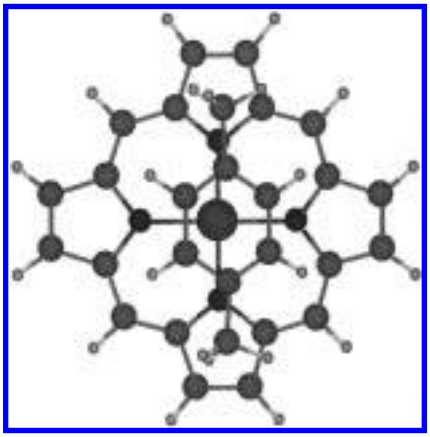

Figure 5. Plane projection of the calculated molecular structure for the [Fe(porphine)(*p*-xylene)]$^+$ cation.

Table 2. Properties Calculated for Iron Porphines Using DFT

	[Fe(porph)]$^+$	[Fe(porph)-(benzene)]$^+$	[Fe(porph)-(toluene)]$^+$	[Fe(porph)-(*p*-xylene)]$^+$
Fe−N (Å)	1.958	1.970 (av)	1.967 (av)	1.967 (av)
N−C_α (Å)	1.379	1.374 (av)	1.374 (av)	1.367 (av)
C_α−C_β (Å)	1.410	1.415 (av)	1.415 (av)	1.415 (av)
C_β−C_m (Å)	1.354	1.351 (av)	1.351 (av)	1.351 (av)
C_α−C_m (Å)	1.365	1.366 (av)	1.367 (av)	1.367 (av)
Cb_1−Cb_2 (Å)[a]	−	1.392	1.391	1.391
Cb_2−Cb_3 (Å)	−	1.386	1.385	1.390
Cb_3−Cb_4 (Å)	−	1.376	1.374	1.383
Cb_4−Cb_5 (Å)	−	1.382	1.392	1.381
Cb_5−Cb_6 (Å)	−	1.376	1.380	1.383
Cb_6−Cb_1 (Å)	−	1.386	1.385	1.390
Fe−C (Å)	−	2.794	2.725, 2.766	2.749
Fe···Ct_P[b] (Å)	0.0	0.19	0.18	0.24
∠P_{24}···Ar[c]	−	14.8°	14.9°	18.6°
BE (kcal/m)	−	−14.4	−16.0	−17.9

[a] Cb_1 and Cb_2 are the coordinated carbon atoms. [b] Ct_P is the center of the mean plane of the 24-atom porphyrin core (P_{24}). [c] Cant angle between the mean plane of the 24-atom porphyrin core and the mean plane of the 6-atom arene ring.

Data for all three complexes are compared in Table 2. The iron atoms are displaced from the porphyrin plane by 0.19 Å for benzene, 0.18 Å for toluene, and 0.24 Å for xylene, reflecting an increasing interaction with increasing basicity of the arene. In the experimental data, on solid-state TPP rather than in vacuo porphine complexes, steric effects apparently lead to the opposite ordering. The average calculated Fe−C distances are 2.79 Å for benzene, 2.72 Å for toluene, and 2.75 Å for *p*-xylene. As with the experimental data, the lack of an homologous trend must result from a competition between electronic effects and local steric effects. The steric effects of the methyl groups are minimized by the electronically desirable nestling of their C−H bonds close to the centers of pyrrole rings. This can be seen for xylene in Figure 5 and is similar in the toluene structure. The planes of the arenes are canted with respect to the porphyrin mean plane by 14.8, 14.9, and 18.6° for benzene, toluene, and xylene, respectively, not very different from those determined experimentally. This suggests that a canting of ca. 15° is an intrinsic feature of the arene/iron porphyrin interaction. Consistent with increasing basicity, the arene binding energies increase in the order benzene < toluene < *p*-xylene, mirroring the trend in Fe atom out-of-plane displacements. The calculations reveal a small alternation of C−C bond lengths in the coordinated arenes, the expected result of some degree of π localization. However, at ca. 0.01 Å, these are at the margins of statistical significance in the experimental data.

The agreement between the calculated and experimental structures is very satisfying. Nevertheless, we decided it would be worthwhile to calculate the effect of a solvating arene on the opposite face of the porphyrin in an [Fe(TPP)(arene)]$^+$ structure. The dimensions of [Fe(porphine)(benzene)]$^+$ were compared with and without solvates held at crystallographically determined positions. Full geometry optimization with a solvating benzene molecule positioned as in **1** gave a structure showing only small changes in the arene−porphine binding parameters. This is not too surprising because, with an arene-to-porphyrin cant angle of 31.1°, the solvating benzene in **1** is not well positioned for good π−π interactions. However, full geometry optimization places the solvating benzene molecule in a nearly coplanar position (cant angle 5°), as found in the *p*-xylene structure **3**. The iron atom is pulled back toward the porphyrin plane (Fe···Ct_p = 0.15 Å), and the Fe−C distances are lengthened to 2.99 Å. This finding supports experimental

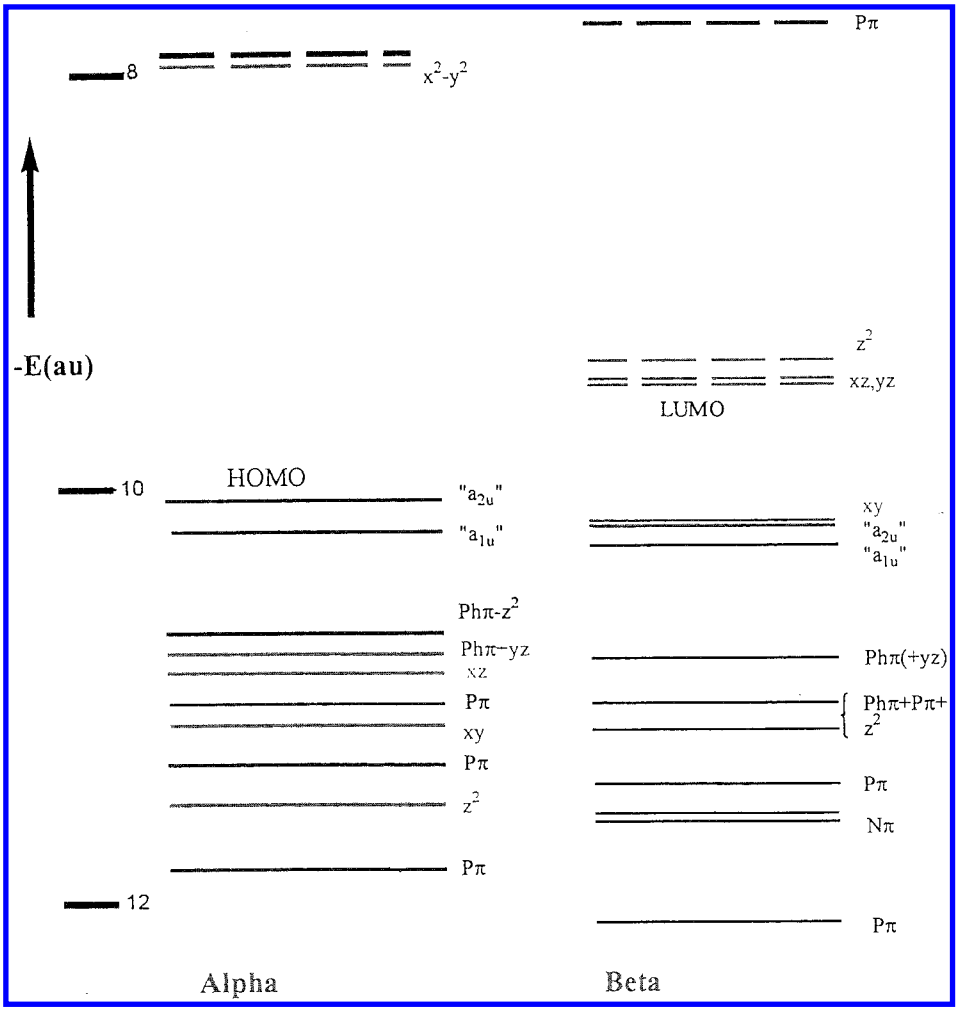

Figure 6. Molecular orbital energy levels for the [Fe(porphine)(benzene)]$^+$ cation.

findings in manganese tetraphenylporphyrin chemistry[21] and has wider significance. It suggests caution in trying to put too fine an interpretation on out-of-plane displacements in metalloporphyrins when the presence or absence of solvation near a vacant site is not taken into account. This comment also applies to the effects of face-to-face orientation in metalloporphyrins.

Molecular Orbitals and Charge Distribution. Ligand field theory predicts the ground-state electronic structure of the [Fe(porphine)]$^+$ cation to be intermediate $S = {}^3/_2$ spin, with $d_{x^2-y^2}$ unoccupied. A spin-unrestricted DFT calculation assigns different spatial orbitals for the different spins, so it can be difficult to directly relate these results to a ligand field model. However, in this case, it is clear that the occupied d orbitals for α spins are z^2, *xy*, *xz*, and *yz*, while for the β spins only the *xy* orbital is occupied. These may be mapped to an $(xy)^2(z^2)^1(xz,yz)^2$ ligand field configuration.

An examination of the form of the molecular orbitals in the [Fe(TPP)(benzene)]$^+$ cation (Figure 6) indicates that the only significant covalent interaction between benzene and iron(III) porphine involves the e_{1g} HOMO of benzene and the d_{z^2} orbital of iron. This bonding interaction with one component of the e_{1g} is illustrated in blue in Figure 7a. For comparison, the interaction of the other component of the e_{1g} with d_{xz} is weak (Figure 7b).

Mulliken population analysis of the charge distribution for the [Fe(TPP)(benzene)]$^+$ cation indicates an overall transfer of charge from the benzene to iron porphine of 0.1992 e. However, there is little change in the electron density at the iron atom upon binding benzene (decreasing slightly from 0.9228 to 0.8725 e), indicating effective charge delocalization over the Fe(porphine) moiety.

The relative contributions of Pauli repulsion, orbital, and electrostatic contributions to the binding energy have been analyzed in terms of iron porphine and benzene fragment orbitals.[36] The Pauli, electrostatic, and orbital contributions to the binding energy of the two unrelaxed fragments are 23.5, −32.5, and −30.6 kcal/mol (total −39.6), respectively. This can be compared with values of 9.7, −19.0, and −14.2 kcal/mol (total −23.5) for the sodium cation−benzene complex and 6.1, −5.3, and −12.8 kcal/mol (total −12.0) for the sodium cation−1,3,5-trifluorobenzene complex.[7] In the sodium cation−arene complexes, it has previously been estimated, from inspection of electrostatic potential maps, that the electrostatic contribution to the binding energy of the sodium ion to benzene and 1,3,5 trifluorobenzene is ca. 60% and 0.0%, respectively. Intriguingly, these variations are mirrored by the "steric repulsion" (the sum of the Pauli and electrostatic terms, which represent ca. 63% and −6% of the binding energy, respectively). In these terms, the benzene−iron porphine complex has a steric repulsion contribution of 23% and thus a significantly higher orbital contribution than for the alkali metal−arene complexes. This covalence is in keeping with the observed benzene−iron d orbital interactions.

C_{60} Coordination to Fe(TPP)$^+$. The interplay of electronic and steric factors in the binding of arenes to Fe(TPP)$^+$ prompted

(36) Morokuma, K. *J. Chem. Phys.* **1971**, *55*, 1236. Ziegler, T.; Rauk, A. *Theor. Chim. Acta* **1977**, *49*, 1. Van den Hoek, P. J.; Kleyn, A. W.; Baerends, E. J. *Comments At. Phys.* **1989**, *23*, 93.

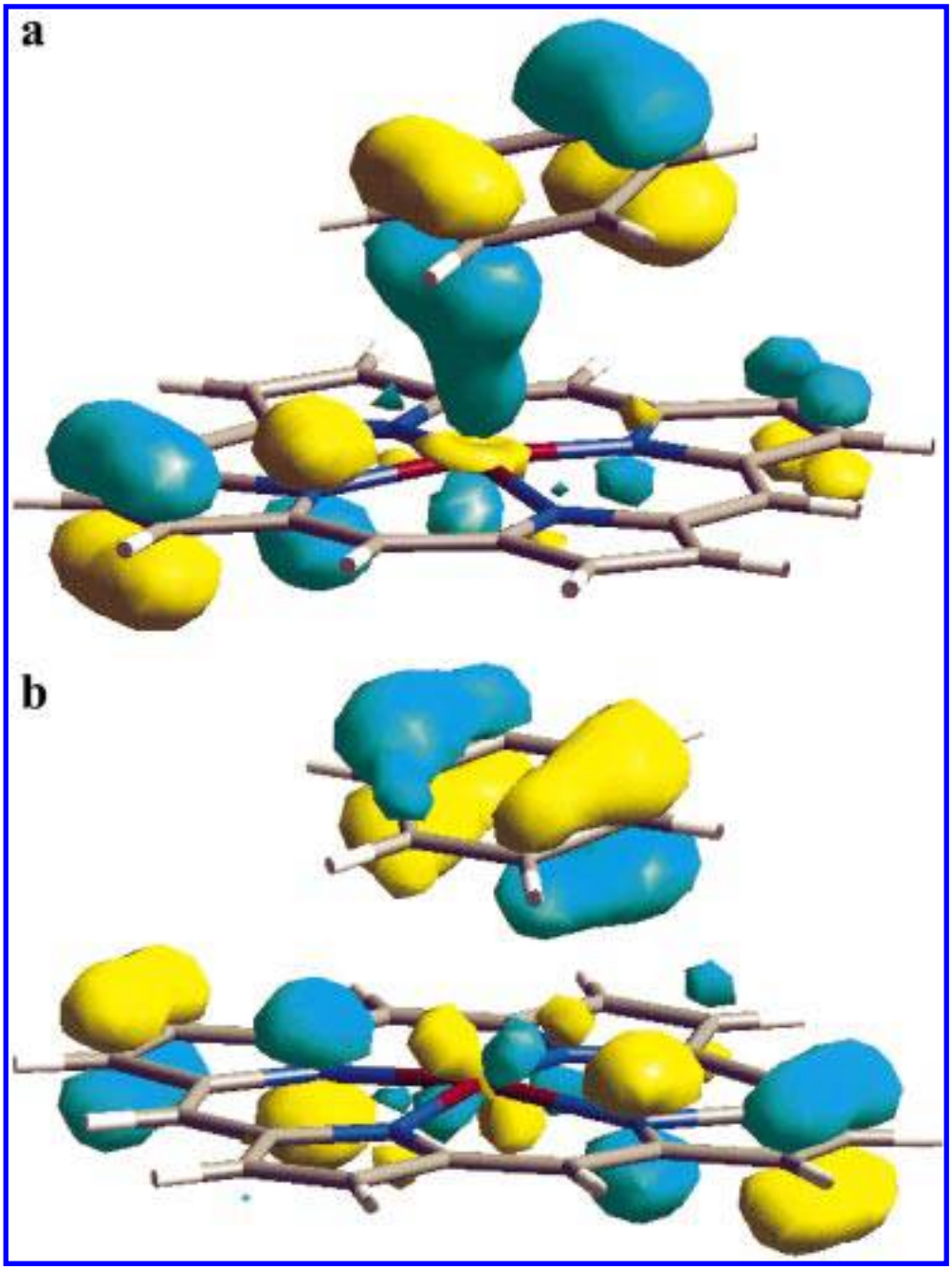

Figure 7. (a) Bonding interaction of one component of the e_{1g} orbital of benzene with d_{z^2} on iron (β spin). (b) Bonding interaction of the other component of the e_{1g} of benzene with d_{xz} on iron (α spin).

us to consider the curved aromatic surface of C_{60} as a comparable ligand. The electron-rich 6:6 ring juncture C−C bonds of C_{60} are less sterically hindered than the C−C bonds of an arene, and coordination of C_{60} to metals is believed to be enhanced by the release of curvature strain.[37] We had explored this possibility earlier with chromium tetraphenylporphyrin complexes, only to find that toluene preferentially crystallized with Cr^{II}(TPP) and that C_{60}^- could not compete with THF solvent for coordination to $Cr^{III}(TPP)^+$.[38] A fairly large number of low-valent transition metal complexes of fullerenes have been reported,[39] and their bonding is generally viewed as covalent. Only while this manuscript was being prepared did the first example with a metalloporphyrin appear, coordination of C_{60} to Ru^{II}(OEP) (OEP = octaethylporphyrinate) being detected by NMR and IR spectroscopy.[40] Ruthenium(II) is a relatively soft, low-valent metal center, so the binding of C_{60} to a hard iron(III) center in the present work represents a potential new class of fullerene−metal coordination. Fullerene interactions with Zn(TPP) are the apparent basis of a chromatographic separation of fullerenes on a stationary phase having Zn(TPP) appended to silica,[41] and a $2Co(OEP)\cdot C_{60}$ cocrystallate has been isolated.[39] However, the fullerene/porphyrin interactions in these situations are not believed to involve metal ligand bonding.

Figure 8 shows the unit cell packing diagram for the X-ray crystal structure of $[Fe(TPP)(C_{60})][F_{20}\text{-}BPh_4]\cdot 2.5$dichlorobenzene (**4**). C_{60} is coordinated to one side of the $Fe(TPP)^+$ cation. On

(37) Haddon, R. C. *J. Comput. Chem.* **1998**, *19*, 139.
(38) Penicaud, A.; Hsu, J.; Reed, C. A. *J. Am. Chem. Soc.* **1991**, *113*, 6698.
(39) Balch, A. L.; Olmstead, M. M. *Chem. Rev.* **1998**, *98*, 2123.
(40) Maruyama, H.; Fujiwara, M.; Tanaka, K. *Chem. Lett.* **1998**, 805.
(41) (a) Xiao, J.; Savina, M. R.; Martin, G. B.; Francis, A. H.; Meyerhoff, M. E. *J. Am. Chem. Soc.* **1994**, *116*, 9341. (b) Xiao, J.; Meyerhoff, M. E. *J. Chromatogr.* **1995**, *715*, 19.

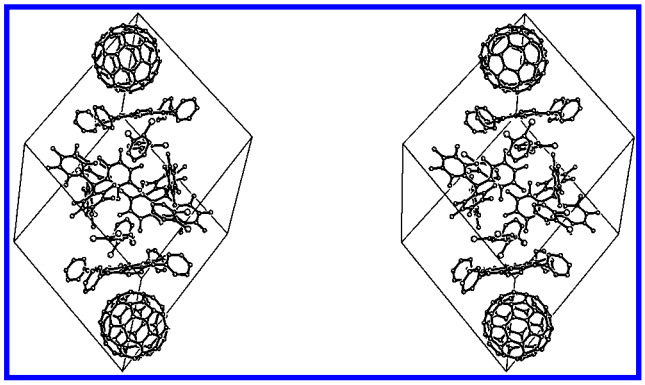

Figure 8. Stereoscopic packing diagram of the unit cell in [Fe(TPP)-(C_{60})][F_{20}-BPh_4]·2.5 dichlorobenzene (**4**).

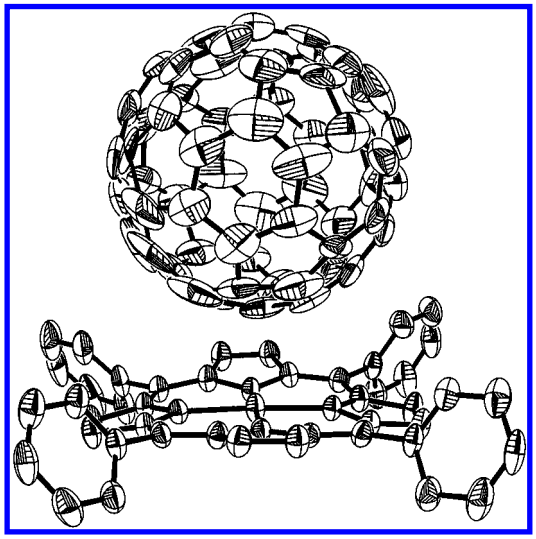

Figure 9. Molecular structure of the $[Fe(TPP)(C_{60})]^+$ cation in **4**.

the other side there is a dichlorobenzene molecule taking a similar solvating role to the noncoordinated arenes seen in **1** and **3**. The remainder of the space is filled by the F_{20}-BPh_4^- anions and further lattice dichlorobenzene molecules. Inspection of stereo packing diagrams reveals two F_{20}-BPh_4^- anions engaged in parallel fourfold fluorophenyl embrace (P4PE), similar to those observed by Scudder and Dance in structures of tetraphenylphosphonium cations.[3]

Figure 9 shows details of the coordination of C_{60} to $Fe(TPP)^+$. When projected onto the porphyrin plane, the coordinated C−C bond is approximately aligned with an N−Fe−N vector of the porphyrin. Unexpectedly, this olefinic 6:6 ring juncture bond is coordinated in an unsymmetrical η^2 fashion: Fe−C(av) = 2.63 and 3.11 Å. This close approach of a carbon atom to Fe is shorter than those in any of the arene complexes **1**−**3** (see Table 1). The approach of C_{60} to the heme is also slightly closer than those in the naturally assembling van der Waals complexes of C_{60} to free-base tetraarylporphyrins (2.70−2.98 Å $\pi-\pi$ separation).[42] This suggests the presence of a covalent Fe−C interaction, and one that is somewhat different from the familiar symmetrical η^2 binding of fullerenes to transition metals. The iron atom is displaced 0.015 Å out of the mean 24-atom porphyrin core and 0.045 Å out of the N4 plane toward the fullerene, also suggestive of some covalent interaction. The Fe-$(TPP)^+$ moiety has essentially the same dimensions as those seen in the arene complexes **1**−**3**, including a similar ruffling of the porphyrin core to **1** and **3**. The magnitude of the saddle

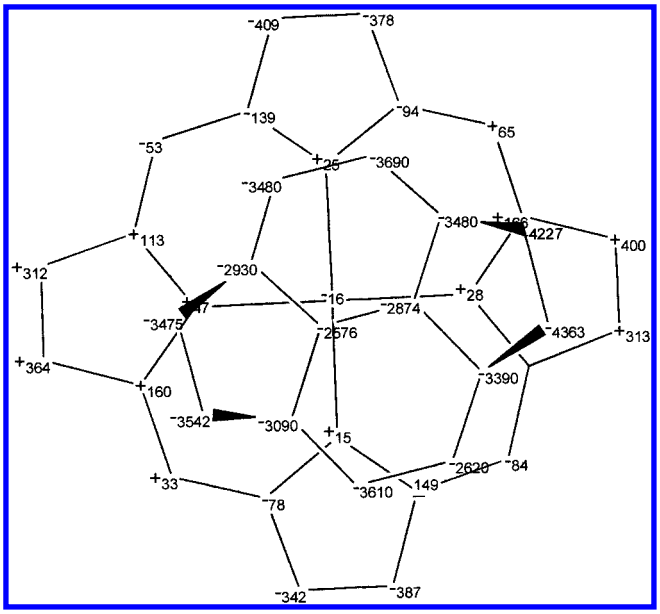

Figure 10. Displacements (in 10^{-3} Å) of atoms from the mean plane of the 24-atom porphyrin core for the $[Fe(TPP)(C_{60})]^+$ cation in **4** together with the 6:6 ring juncture C atoms of C_{60} that are coordinated.

type ruffling in **4** is, however, considerably greater than that in **1** or **3**. The appropriate displacement diagram is shown in Figure 10 for comparison to Figure 4. The average displacements for the C_α, C_β, and C_{meso} atoms are 0.115, 0.360, and 0.057 Å, respectively, compared to 0.017, 0.039, and 0.028 Å for **1**, 0.103, 0.180, and 0.180 for $Fe(OClO_3)(TPP)$,[43] and 0.390, 1.079, and 0.050 Å for the heavily distorted Zn(MeOH)(OETPP).[44]

The structure of $[Fe(TPP)(C_{60})]^+$ presages a new class of fullerene complexes and bonding modes that remain to be fully understood. In the cocrystallate $2Co(OEP)\cdot C_{60}$, where face-to-face Co(OEP) dimers sandwich C_{60} units in an infinite chain structure, metal−fullerene covalent bonding is believed to be absent.[39] This is based on the long Co−C distances (2.7−2.9 Å) and the absence of an out-of-plane displacement of the cobalt atom. An alternate view is that the cobalt is weakly six-coordinate with balancing Co−C and Co−N interactions (the latter from the face-to-face porphyrin dimer). One interesting observation about **4** concerns its color. Unlike van der Waals fullerene/porphyrin conjugates, which retain the purple colors of the individual chromophores,[42] crystals of **4** are green. This indicates fullerene-to-iron charge transfer and is consistent with some degree of covalent Fe−C bonding. Such charge-transfer complexes are of interest with respect to possible new organic conductors.[45]

Conclusion. This work establishes a covalent component to the weak binding of arenes to iron(III) porphyrin cations. A similar situation with fullerenes is likely. It requires that benzene should be considered a bone fide ligand, even to such hard metals as Fe(III). This complexation has distinctive structural features that differentiate it from $\pi-\pi$ solvation or a purely electrostatic attraction, although it is likely there is a continuum of interactions between these definitional ideals. The M−C distances and cant angles of Co(F_{28}-TPP)·2toluene,[46] Mn(TPP)·

(42) Boyd, P. D. W.; Hodgson, M. C.; Rickard, C. E. F.; Oliver, A. G.; Brothers, P. J.; Bolskar, R. D.; Reed, C. A. *J. Am. Chem. Soc.*, in press.

(43) Reed, C. A.; Mashiko, T.; Bentley, S. P.; Kastner, M. E.; Scheidt, W. R.; Spartalian, K.; Lang, G. *J. Am. Chem. Soc.* **1979**, *101*, 2948.

(44) Barkigia, K. M.; Berber, M. D.; Fajer, J.; Medforth, C. J.; Renner, M.; Smith, K. M. *J. Am. Chem. Soc.* **1990**, *112*, 8851.

(45) Martín, N.; Sánchez, L.; Illescas, B.; Pérez, I. *Chem. Rev.* **1998**, *98*, 2527.

(46) Smirnov, V. V.; Woller, E. K.; DiMagno, S. G. *Inorg. Chem.* **1998**, *37*, 4971.

Table 3. Crystal Data and Structure Refinement Information for Compounds **1**, **2**, and **4**

identification code	$[FeTPP(C_6H_6)][CB_{11}H_6Br_6]\cdot 3.5C_6H_6$ (**1**)	$[FeTPP(C_7H_8)][CB_{11}H_6Cl_6]\cdot 2C_7H_8$ (**2**)	$[FeTPP(C_{60})][B(C_6F_5)_4]\cdot 2.5C_6H_4Cl_2$
empirical formula	$C_{72}H_{61}B_{11}Br_6FeN_4$	$C_{66}H_{58}B_{11}Br_6FeN_4$ (??)	$C_{137}H_{38}BF_{20}FeCl_5N_4$
formula weight	1636.50	1561.41	2363.72
temperature, K	158(2)	173(2)	203(2)
wavelength, Å	0.710 73	0.710 73	0.710 73
crystal system, space group	triclinic, $P\bar{1}$	triclinic, $P\bar{1}$	triclinic, $P\bar{1}$
unit cell dimensions			
a, Å	13.4685(7)	13.877(3)	14.4297(2)
b, Å	13.7905(7)	13.916(4)	18.2913(3)
c, Å	19.4425(10)	15.989(3)	20.4113(2)
α, deg	106.5120(10)	105.31(2)	75.711(1)
β, deg	92.1570(10)	95.720(10)	75.303(1)
γ, deg	94.5300(10)	100.06(2)	74.335(1)
volume, Å^3	3444.6(3)	2897.5(12)	4924.68(20)
Z, calcd density, Mg/m^3	2, 1.578	2, 1.417	2, 1.390
absorption coefficient, mm^{-1}	3.745	0.583	0.457
F(000)	1624	1262	2053.7
crystal size, mm	0.23 × 0.16 × 0.13	0.6 × 0. 7 × 0.4	0.4 × 0.3 × 0.15
θ range (data collection), deg	1.09−28.36	1.34−23.63	1.0−25.0
limiting indices	$-17 \le h \le 17$ $-18 \le k \le 18$ $-25 \le l \le 25$	$-13 \le h \le 13$ $-13 \le k \le 13$ $-16 \le l \le 15$	$-16 \le h \le 17$ $-20 \le k \le 21$ $0 \le l \le 24$
no. of reflections collected/unique	34 298/15 648 [$R_{int} = 0.0563$]	7218/6230 [$R_{int} = 0.027\,21$]	45 498/19 665 [$R_{int} = 0.0321$]
absorption correction	semiempirical via SADABS	semiempirical via Ψ-Scans	semiempirical via SADABS
max/min transmission	0.624 898/0.487 799	0.934/0.847	0.9347/0.8385
refinement method	full-matrix least-squares on F^2	full-matrix least-squares on F^2	full-matrix least-squares on F^2
data/restraints/parameters	15 645/0/842	6227/0/708	17 152/1387/1955
goodness-of-fit on F^2	1.034	1.100	1.015
rinal *R* indices [$I > 2\sigma(I)$]	$R_1 = 0.0565$ $wR_2 = 0.0882$	$R_1 = 0.0561$ $wR_2 = 0.1498$	$R_1 = 0.0926$ $wR_2 = 0.2586$
R indices (all data)	$R_1 = 0.1080$ $wR_2 = 0.1083$	$R_1 = 0.0711$ $wR_2 = 0.1681$	$R_1 = 0.1265$ $wR_2 = 0.2957$
extinction coefficient		0.0151(12)	
largest diff peak and hole, e Å^{-3}	0.598 and −0.666	0.936 and −0.652	2.152 and −1.269

2toluene,[47] and Co(F_{20}-TPP)·benzene[48] (3.05, 3.05, and 3.09 Å, and 11.9°, 10.7°, and 6.0° respectively) suggest a progression of decreasing covalence toward the van der Waals ideal.

In a broader context, this study suggests that solvents such as benzene must be considered as potential ligands in any situation where coordinatively unsaturated cations are generated. Indeed, the recent characterization of a heptane complex of an iron(II) porphyrin[49] suggests there is really no such thing as a noncoordinating solvent. Many vacant coordination sites in solution-phase chemistry are best viewed as convenient fictions unless solvent molecules are physically excluded by steric effects. One suspects that in even the simplest of Lewis acid−base adducts, there is covalence in the interaction. Certainly the rather common use in supramolecular chemistry of the term "noncovalent" to describe entities brought together with metal−ligand bonds[50] must be viewed as potentially misleading. The term "coordinatively bonded" is preferable.

Experimental Section

Synthesis. All manipulations were carried out under anhydrous conditions in an inert atmosphere glovebox. Fe(TPP)($CB_{11}H_6Br_6$) was prepared by oxidizing Fe(TPP) with 1 equiv of $[N(C_6H_4Br)_3][CB_{11}H_6Br_6]$ in a refluxing solution of benzene.[23] Crystals of $[Fe(TPP)(C_6H_6)][CB_{11}H_6Br_6]\cdot 3.5C_6H_6$ (**1**) suitable for X-ray analysis were grown from 10 mM solutions of benzene-d_6 over a 2-month period. $[Fe(TPP)(C_7H_8)][CB_{11}H_6Cl_6]\cdot 2C_7H_8$ (**2**) was prepared by metathesis with Fe(TPP)(Br) and $Ag(CB_{11}H_6Cl_6)$ in refluxing toluene. The precipitated AgBr was removed by filtration through a medium- then a fine-porosity frit, and crystals suitable for X-ray analysis were grown by slow evaporation. $[Fe(TPP)][F_{20}\text{-}BPh_4]$ was prepared by metathesis of Fe(TPP)Br with $Et_3Si[F_{20}\text{-}BPh_4]$[51] in *o*-dichlorobenzene and isolated by precipitation with hexane. $[Fe(TPP)(C_{60})][F_{20}\text{-}BPh_4]$ was prepared by mixing $[Fe(TPP)][F_{20}\text{-}BPh_4]$ with 1 equiv of C_{60} in a minimal amount of *o*-dichlorobenzene. Hexane was added to precipitate the crude product. Crystals of $[Fe(TPP)(C_{60})][F_{20}\text{-}BPh_4]\cdot 2.5$dichlorobenzene (**4**) suitable for X-ray crystallography were obtained by layering a concentrated *o*-dichlorobenzene solution with hexanes in an 11-mm-diameter sealed glass tube.

Computational Details. Density functional calculations were performed using the Amsterdam Density Functional program.[52] Double-ζ Slater-type basis sets were used for C(2s,2p), N(2s,2p), and H(1s) augmented by a single 3d polarization function. A triple-ζ basis set was used for Fe(3s,3p,3d,4s). The inner electron configurations were assigned to the core and were treated using the frozen core approximation. All calculations were carried out using the local density approximation due to Vosko, Wilk, and Nusair,[53] with nonlocal corrections for exchange due to Becke,[54] with nonlocal corrections for correlation due to Lee, Yang, and Parr.[55] Full geometry optimizations were carried out for the $[Fe(porphine)]^+$ cation together with the benzene, toluene, and *p*-xylene adducts. A symmetry-constrained optimization for $[Fe(porphine)]^+$ and $[Fe(TPP)(benzene)]^+$ using D_{4h} and C_s symmetry, respectively, gave the same structures and energies as the unconstrained

(47) Kirner, J. F.; Reed, C. A.; Scheidt, W. R. *J. Am. Chem. Soc.* **1977**, *99*, 1093.
(48) Kadish, K. M.; Araullo-McAdams, C.; Han, B. C.; Frazen, M. M. *J. Am. Chem. Soc.* **1990**, *112*, 8364.
(49) Evans, D. R.; Drovetskaya, T.; Bau, R.; Reed, C. A.; Boyd. P. D. W. *J. Am. Chem. Soc.* **1997**, *119*, 3633.
(50) For a recent example, see: Armaroli, N.; Diederich, F.; Echegoyen, L.; Habicher, T.; Flamigni, L.; Marconi, G.; Nierengarten, J.-F. *New. J. Chem.* **1999**, 77.
(51) Lambert, J. B.; Zhang, S.; Ciro, S. M. *Organometallics* **1994**, *13*, 2430.
(52) (a) ADF 2.3.0, Theoretical Chemistry, Vrije Universiteit, Amsterdam. (b) Baerends, E. J.; Ellis, D. E.; Ros, P. *Chem. Phys.* **1973**, *2*, 41. (c) te Velde, G.; Baerends, E. J. *J. Comput. Phys.* **1992**, *99*, 84.
(53) Vosko, S. H.; Wilk, L.; Nusair, M. *Can. J. Phys.* **1980**, *58*, 1200.
(54) Becke, A. D. *Phys. Rev. A* **1988**, *38*, 3098.
(55) Lee, C.; Yang, W.; Parr, R. G. *Phys. Rev. B* **1988**, *37*, 785.

calculation. All open-shell calculations were spin unrestricted, with a spin quartet ($S = {}^3/_2$) ground state.

Crystallography. The single-crystal X-ray data collection for **1** was performed on a Siemens P4/CCD diffractometer using Mo Kα radiation at −115 °C by Dr. Joseph W. Ziller at the University of California, Irvine. The structure was solved by direct methods using SHELXTL version 5.1[56] and refined on F^2 by full-matrix least-squares techniques, giving a final R_1 value of 5.65% on 10 136 reflections, with $I > 2\sigma(I)$ ($R_1 = 10.8$ (all data)). All atoms, except the hydrogens, were refined anisotropically, giving acceptable U_{ij} values. The hydrogens were located upon refinement but were allowed to refine using the riding atom model. Data for **2** were collected using a Siemens $P2_1$ diffractometer using Mo Kα radiation at a temperature of −100 °C at the University of Southern California. The structure was solved using direct methods as described for **1**, with the exception that not all hydrogens were located by refinement. The final *R*-factor was 5.61% on 5147 reflections, with $I > 2\sigma(I)$ ($R_1 = 7.11\%$ (all data)). Data for **4** were obtained on a Siemens SMART diffractometer with a CCD area detector using Mo Kα radiation at a temperature of −70 °C at The University of Auckland. The structure was solved by direct methods using SHELXS-97[57] and refined on F^2 using SHELXL-97.[58] Hydrogen atoms on the porphyrin molecule were incorporated at calculated positions and included in the final refinement using a riding atom model. The iron porphyrin and tetra(pentafluorophenyl)borate moieties were clearly defined in difference density maps. While the position of the fullerene was clear, it was apparent that it was disordered. In this structure, it was possible to resolve two C_{60} moieties, and these were refined under bond length constraint. Three 1,2-dichlorobenzene solvent molecules were identified from difference density maps. All were refined using rigid groups for the benzene ring. The final *R*-factor was 9.4% on 11 847 reflections, with $I > 2\sigma(I)$ ($R_1 = 12.7\%$ (all data)). It was apparent that one solvent molecule was only half-occupied. While the final refinement was satisfactory, it was apparent that the dichlorobenzene solvent molecules were not well defined. To further investigate this, the SQUEEZE function of the program PLATON[59,60] was used to examine the dichlorobenzene-containing cavities. It was found that the total electron density in these cavities corresponded well to 2.5 dichlorobenzene molecules. A refinement using reflections modified by the SQUEEZE procedure behaved well, and the geometries of the fullerene, iron porphyrin, and borate anion were in good agreement with the model above incorporating the dichlorobenzene molecules, although, of course, the *R*-factors were significantly reduced. Essential crystal and refinement data are given in Table 3. Full details are available in the Supporting Information.

Acknowledgment. We are grateful for support from the National Institutes of Health (GM 23851), the Marsden Fund of the Royal Society of New Zealand (UOA613), and The University of Auckland Research Committee.

Supporting Information Available: Details of the X-ray crystal structure determinations (PDF). This material is available free of charge via the Internet at http://pubs.acs.org.

JA9910816

(56) Sheldrick, G. M. Bruker AXS: Madison, WI, 1997.
(57) Sheldrick, G. M. SHELXS97, A Program for Crystal Structure Solution; University of Göttingen, Germany, 1997.
(58) Sheldrick, G. M. SHELXL97, A Program for Crystal Structure Refinement; University of Göttingen, Germany, 1997.
(59) Spek, A. L. *Acta Crystallogr.* **1990**, *A46*, C34.
(60) Sluis, P. V. D.; Spek, A. L. *Acta Crystallogr.* **1990**, *A46*, 194.